Preparation, Structure, and Properties of Symmetrically 1,3-Difunctionalized Penta- and Hexafluorobicyclo[1.1.1]pentanes

Michael D. Levin,[†] Steven J. Hamrock,[‡] Piotr Kaszynski,[§] Alexander B. Shtarev,[†] Galina A. Levina,[†] Bruce C. Noll,[†] Martin E. Ashley,[†] Richard Newmark,[⊥] George G. I. Moore,[⊥] and Josef Michl*,[†]

Contribution from the Department of Chemistry and Biochemistry, University of Colorado, Boulder, Colorado 80309-0215, and 3M Company, Saint Paul, Minnesota 55144

Received April 3, 1997[⊗]

Abstract: Exhaustive direct fluorination of dimethyl bicyclo[1.1.1]pentane-1,3-dicarboxylate leads to dimethyl pentafluorobicyclo[1.1.1]pentane-1,3-dicarboxylate (**2**) and hexafluorobicyclo[1.1.1]pentane-1,3-dicarboxylate (**3**). The latter was hydrolyzed to the diacid (**4**) and converted to the 1,3-dibromo and 1,3-diiodo analogues (**5** and **6**) by the Hunsdieker reaction followed by treatment with SmI_2. Na/NH_3 reduction of the disodium salt **10** causes cage C−C bond cleavage. Single-crystal X-ray diffraction analysis of **3** revealed very short nonbonded F−F separations of 2.41 Å and an interbridgehead distance of 1.979 Å, long compared with 1.875 Å in 1,3-diacetylbicyclo[1.1.1]-pentane [**19**; cf. 1.954 Å calculated (MP2/6-31G*) for 2,2,4,4,5,5-hexafluorobicyclo[1.1.1]pentane (**13**)]. Calculation suggests a strain energy of 101 kcal/mol (MP2/6-31G*) for the hexafluorinated cage, compared with 68 kcal/mol for the parent bicyclo[1.1.1]pentane (**20**). The remarkably low pK_a values of **4** [0.73 and 1.34; cf. 3.22 and 4.26 for the parent diacid **24**] originate in a direct field effect of fluorine atoms, combined with an increased s character of the exocyclic hybrid orbital on the bridgehead carbon in **4** (calculated 34% in **13**) relative to **24** (calculated 30% in **20**). Analysis of the strongly coupled nuclear spin systems of **2** and **3**, based on a combination of two-dimensional NMR, spectral simulations, and GIAO-HF/6-31G* calculations of chemical shifts, revealed large and stereospecific long-range $^1H-^{13}C$, $^1H-^{19}F$, $^{13}C-^{19}F$, and $^{19}F-^{19}F$ spin−spin coupling constants.

Introduction

There are several reasons for which the presently unknown analogues of [*n*]staffanes (**1**) fluorinated on the bridge carbons

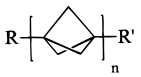

1

would be useful to synthesize and investigate. First, their bridgehead hydrogens might be sufficiently acidic for direct functionalization, facilitating attempts to use these rodlike molecules as modules in molecular-size construction sets.[1] Second, it would be interesting to compare the properties of fluorinated oligomeric or polymeric [*n*]staffanes with those of the parent [*n*]staffanes. Among others, we would like to evaluate the effects of fluorination on electronic interaction through these relatively rigid spacers, e.g., on the long-range propagation of spin density from a terminal bridgehead position.[2] Third, the fluorine atoms present in the neighboring bridges of the bicyclo[1.1.1]pentane cage are forced to be much closer than the sum of their van der Waals radii, and it would be interesting to see how the crowding is accommodated, what effect it has on cage strain, and whether any unusual reactivity or spectral properties might result from the nonbonded interactions.

Chart 1. Bicyclo[1.1.1]pentanes

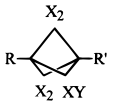

	R	R'	X	Y
2	$COOCH_3$	$COOCH_3$	F	H
3	$COOCH_3$	$COOCH_3$	F	F
4	COOH	COOH	F	F
5	Br	Br	F	F
6	I	I	F	F
7	$COOCH_3$	$COOCH_3$	H	H
8	Br	I	F	F
9	H	I	F	F
10	COONa	COONa	F	F
13	H	H	F	F
19	$COCH_3$	$COCH_3$	H	H
20	H	H	H	H
21	H	H	F	H
24	COOH	COOH	H	H
27	COOH	H	H	H
28	COOH	H	F	F

We have started by investigating the first member of the series (**1**, $n = 1$) and now report that (i) dimethyl pentafluorobicyclo-[1.1.1]pentane-1,3-dicarboxylate (**2**) and dimethyl hexafluoro-

[†] University of Colorado.
[‡] Present address: 3M Company.
[§] Present address: Department of Chemistry, Vanderbilt University, Nashville, TN 37235.
[⊥] 3M Company.
[⊗] Abstract published in *Advance ACS Abstracts,* December 15, 1997.
(1) Kaszynski, P.; Friedli, A. C.; Michl, J. *J. Am. Chem. Soc.* **1992**, *114*, 601.
(2) McKinley, A. J.; Ibrahim, P. N.; Balaji, V.; Michl, J. *J. Am. Chem. Soc.* **1992**, *114*, 10631.

S0002-7863(97)01051-2 CCC: $14.00 © 1997 American Chemical Society

bicyclo[1.1.1]pentane-1,3-dicarboxylate (**3**) are accessible by direct fluorination, albeit in moderate yields, and that the latter is easily converted via the diacid **4** into the symmetrically 1,3-dihalogenated hexafluorobicyclo[1.1.1]pentanes **5** and **6** and degraded to cyclobutane derivatives under strongly reducing conditions, (ii) all nine atoms in the CF_2 groups of **3** lie in a single plane, with very short F−F nonbonded distances, the bridgehead-to-bridgehead distance is significantly longer than in the hydrogenated parent, and calculations suggest very high steric strain, (iii) the pK_a values of **4** suggest that the classical field effect on carboxyl acidity is important in spite of the apparently unfavorable orientation of the CF dipoles, and that changes in the hybridization at the bridgehead carbon play a role, and (iv) the $^1H-^{13}C$, $^1H-^{19}F$, $^{13}C-^{19}F$, and $^{19}F-^{19}F$ spin−spin coupling constants deduced from the NMR spectra of **2** and **3** are highly stereospecific and many are unusually large. The assignment of the NMR spectra of **2** was not obvious and was only arrived at upon comparison with *ab initio* calculations of chemical shifts. It is compatible with results independently obtained for **3**.

Results and Discussion

Direct Fluorination. Successful direct fluorination of various polycyclic hydrocarbons (norbornane,[3] bicyclo[2.2.2]octane,[4] adamantane,[5] diamantane,[6] and bisnoradamantane[7]) has been reported. However, according to a preliminary report[7] ring opening was observed during attempted direct fluorination of [1.1.1]propellane and cubane, presumably because of their highly strained nature. Thus, it was not clear whether the very high strain in the bicyclo[1.1.1]pentane cage (68 kcal/mol[8]) will not cause difficulties. Successful radical chlorination of bicyclo-[1.1.1]pentanes has been reported.[9] When both bridgeheads were blocked, it produced 2,2-dichloro derivatives smoothly, but attempted perchlorination under forcing conditions caused cage degradation.[9a]

Dimethyl bicyclo[1.1.1]pentane-1,3-dicarboxylate (**7**)[10] was subjected to direct fluorination.[11] After workup with methanol, the main product was **3** (40%), with a significant amount of **2**, and smaller amounts of less completely fluorinated materials, which were not isolated.

Functional Group Transformations. The hydrolysis of the diester **3** to the free diacid **4** (Scheme 1) presented no difficulties. The Hunsdieker reaction of the diacid proceeded well under standard conditions to give a 68% yield of the dibromide **5**. In contrast, all attempts at decarboxylative iodination using common procedures[12] failed.

However, a reaction of **5** with samarium diiodide in tetrahydrofuran produced the diiodide **6** in a yield of 31%. The yield is best when 1 equiv of SmI_2 is added slowly. The buildup and disappearance of an intermediate product, 1-bromo-3-iodohexafluorobicyclo[1.1.1]pentane (**8**), was followed by GC−MS and ^{19}F NMR spectroscopy, but no attempt was made to isolate it. Excess SmI_2 is to be avoided, as it converts **5** to a material whose spectra fit the structure of 1-iodo-2,2,4,4,5,5-hexafluorobicyclo[1.1.1]pentane (**9**).

Scheme 1. Fluorination and Functional Group Transformations

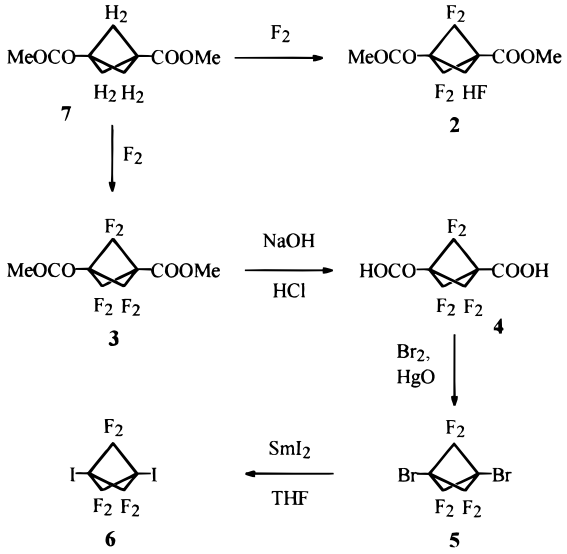

Electron transfer from Sm(II) to **5** with a concomitant loss of Br^- to yield a bridgehead radical capable of abstracting an iodine atom from SmI_2 (or a hydrogen atom from the solvent) is a reasonable mechanistic possibility. Another plausible mechanism is a halogen exchange in a complex of **5** with SmI_2. Other possiblities cannot be excluded at this time. Treatment with SmI_2 may represent a general reaction for the conversion of bridgehead bromides to iodides, and needs to be explored further.

Reduction of Disodium Hexafluorobicyclo[1.1.1]pentane-1,3-dicarboxylate (10). Reductive dehalogenation of the hexafluorobicyclo[1.1.1]pentane cage was attempted as a potentially selective synthetic route to partially fluorinated bicyclo-[1.1.1]pentane derivatives. Although perfluorinated hydrocarbons are extremely stable toward reduction, powerful electron-transfer reducing agents, such as solutions of alkali metals in ammonia and some radical anions, can defluorinate them.[13]

Several attempts to reduce **10** with sodium naphthalenide and sodium−benzophenone ketyl did not yield any detectable product,[14] and the starting material was recovered. Two products were obtained in a total yield of 34% when **10** was reduced with a solution of sodium in liquid ammonia. After acidification and esterification, they were separated by preparative GC. They have very similar NMR spectra,[15] and their structures were assigned as the cis (**11**) and the trans (**12**) isomers of dimethyl 1-(difluoromethyl)cyclobutane-1,3-dicarboxylate. The stereochemistry was determined by single-crystal X-ray diffraction analysis.[15] A precedent for this C−C bond cleavage can be seen in the reported[16] reduction of a benzylic

(3) Campbell, S. F.; Stephens, R.; Tatlow, J. C. *Tetrahedron* **1965**, *21*, 2997.
(4) Adcock, J. L.; Zhang, H. Unpublished results, quoted in ref 7.
(5) (a) Moore, R. E.; Driscoll, G. L.; *J. Org. Chem.* **1978**, *43*, 4978. (b) Robertson, G.; Liu, E. K. S.; Lagow, R. J. *J. Org. Chem.* **1978**, *43*, 4981. (c) Adcock, J. L.; Robin, M. L. *J. Org. Chem.* **1983**, *48*, 3128.
(6) (a) Adcock, J. L.; Luo, H. *J. Org. Chem.* **1992**, *57*, 2162. (b) Wei, H.-C.; Corbelin, S.; Lagow, R. J. *J. Org. Chem.* **1996**, *61*, 1643.
(7) Adcock, J. L.; Zhang, H. *J. Org. Chem.* **1996**, *61*, 1975.
(8) Wiberg, K. B. *Angew. Chem., Int. Ed. Engl.* **1986**, *25*, 312.
(9) (a) Robinson, R. E.; Michl, J. *J. Org. Chem.* **1989**, *54*, 2051. (b) Wiberg, K. B.; Williams, V. Z. *J. Org. Chem.* **1970**, *35*, 369.
(10) Kaszynski, P.; Michl, J. *J. Org. Chem.* **1988**, *53*, 4593.
(11) (a) Moore, G. G. I.; Guerra, M. A. U.S. Patent 5 476 974, Dec 19, 1995. (b) Costello, M. G.; Moore, G. G. I. U.S. Patent 5 286 880, Feb 15, 1994, Example 6.
(12) (a) Abeywickrema, R. S.; Della, E. W. *J. Org. Chem.* **1980**, *45*, 4226. (b) Moriarty, R. M.; Khosrowshahi, J. S.; Dalecki, T. M. *J. Chem. Soc., Chem. Commun.* **1987**, 675. (c) Della, E. W.; Taylor, D. K. *Aust. J. Chem.* **1991**, *44*, 881.
(13) Smart, B. E. In *Organofluorine Chemistry: Principles and Commercial Applications*; Banks, R. E., *et al.*, Eds.; Plenum Press: New York, 1994; p 57 and references cited therein.
(14) No fluoride anions were detected by ^{19}F NMR in the worked up reaction mixtures from these experiments. Defluorination of perfluorocarbons may yield colloidal solutions of elemental carbon and fluoride (for an example see: Marsella, J. A.; Gilicinski, A. G.; Couglin, A. M.; Pez, G. P. *J. Org. Chem.* **1992**, *57*, 2856).
(15) See the Supporting Information.

Scheme 2. Proposed Mechanism for Reduction of **10**

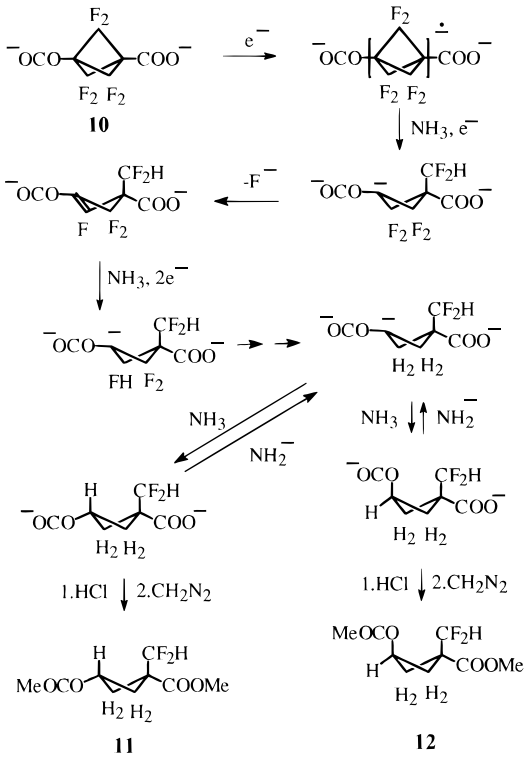

bond in 2-phenylbicyclo[1.1.1]pentane upon treatment with excess sodium in liquid ammonia, which yields benzylcyclobutane.

The mechanism of the reductive cleavage of a C−C bond in **10** is of interest. A plausible proposal is outlined in Scheme 2. An extra electron is initially accepted into an orbital of σ^*_{C-C} character. RHF/6-31G* calculations on a model system, 2,2,4,4,5,5-hexafluorobicyclo[1.1.1]pentane (**13**), confirm that the LUMO is localized mainly on carbon atoms of the cage, and has a node across each C−C bond. Cleavage of one of the six CC bonds followed by further reduction and protonation generates a CHF_2 group, inert to reduction, and a cyclobutane ring carrying four fluorine atoms in position β to a carboxylate enolate. A sequence of repeated β-elimination, double bond reduction, and protonation steps completes the process. These fluorine loss steps apparently occur much faster than the initial CC bond cleavage, since no products with a partially fluorinated cyclobutane ring were detected. The formation of the two stereoisomers is presumably the outcome of a kinetically controlled final protonation step. Under the reaction conditions, product epimerization is relatively slow, but over a period of hours, the portion of the cis isomer in the strongly basic reaction mixture grows from about 60% to nearly 100%.

Molecular Geometry. The way in which the hexafluorinated bicyclo[1.1.1]pentane cage solves the potentially severe problem of fluorine atom crowding (the standard van der Waals radius of the fluorine atom is 1.47 Å[13,17]) strikes us as particularly interesting. The geometry of **3** was determined by X-ray diffraction on a single crystal. The distances and angles for the major component of a disordered structure are shown in Figure 1. In order to obtain a nearly flat final difference map, two alternative sets of positions for carbons in the cage core were refined. Final site occupancies were 0.91 for the principal site and 0.09 for the minor site.[15] A thermal ellipsoid plot of the principal site is shown in Figure 2.

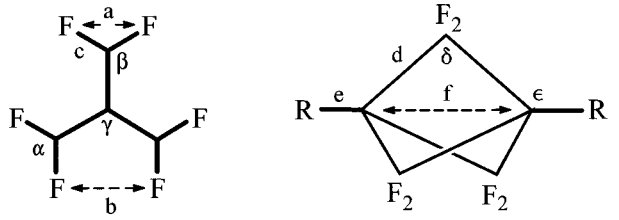

R = $COOCH_3$ (**3**); H (**13**); $COCH_3$ (**19**)

Distance Å	**3**[a] Obsd	**13** Calcd	**19**[a,b] Obsd	Angle deg	**3**[a] Obsd	**13** Calcd	**19**[a,b] Obsd
a	2.159	2.155	–	α	106.51	105.4	–
b	2.411	2.495	–	β	117.58	118.0	–
c	1.347	1.354	–	γ	84.18	84.2	88.1
d	1.562	1.554	1.547	δ	78.57	78.5	74.2
e	1.503[c]	1.089[d]	1.493[c]	ϵ	129.28	129.3	127.4
f	1.979	1.967	1.875				

[a] Average values (except **f**) from X-ray diffraction. [b] Hydrogens in place of fluorines. [c] C-C distance. [d] C-H distance.

Figure 1. Molecular geometries of **13** (calcd, MP2/6-31G*), **3**, and **19** (obsd).

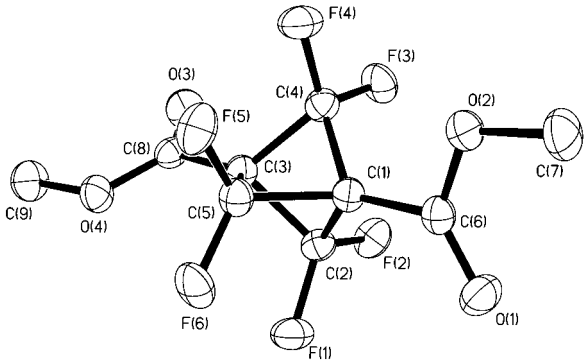

Figure 2. Thermal ellipsoid plot of the principal site of **3**.

The six fluorines and the three bridge carbons of the cage are coplanar. The two bridgehead carbons and the two carboxylic carbons lie on an approximate 3-fold axis of symmetry, perpendicular to the plane of the fluorines. The deviations of the cage carbon atoms from 3-fold symmetry are larger than the deviations of the fluorine atoms. The largest deviation in CC bond lengths exceeds the error of measurement by a factor of 3. At 2.159 Å the geminal fluorines are closer to each other than the proximate ones (four bonds apart, 2.411 Å), but the latter are still about 0.5 Å closer to each other than the sum of the van der Waals radii. The distance between geminal fluorines is very close to the value observed for numerous ordinary geminal difluoro compounds,[18] and is in excellent agreement with the fluorine nonbonded radius of 1.08 Å postulated by Bartell.[19]

The structural parameters of selected geminally difluorinated hydrocarbons are listed in Table 1. At 1.347 Å, the C−F bonds in **3** are shorter than those in 2,2-difluoropropane (**14**; 1.370 Å)[20] and are similar in length to those in perfluoropropane (**15**; 1.34 Å) and in 1,1-difluorocyclopropane (**16**; 1.355 Å),[21] but

(16) Wiberg, K. B.; Ross, B. S.; Isbell, J. J.; Mc Murdie, N. *J. Org. Chem.* **1993**, *58*, 1372.
(17) Bondi, A. *J. Phys. Chem.* **1964**, *68*, 441.
(18) Glidewell, C.; Meyer, A. Y. *J. Mol. Struct.* **1981**, *72*, 209 and references cited therein.
(19) Bartell, L. S. *J. Chem. Phys.* **1960**, *32*, 827.
(20) Mack, H.-G.; Dakkouri, M.; Oberhammer, H. *J. Phys. Chem.* **1991**, *95*, 3136.

Table 1. Comparison of Experimental Bond Lengths and Valence Angles in Geminally Difluorinated Hydrocarbons

molecule	*r*(CF) Å	*r*(C−CF_2) Å	∠FCF (deg)	∠C−CF_2−C (deg)	ref
14	1.370	1.512	106.2	115.3	20
15	1.34[a]	1.55	109.3[a]	115.9	8
16	1.355	1.464	108.4	64.1	21
17	1.314	1.505	112.2	60.0	22
18	1.335	1.526	109.9	89.3	23
18	1.324	1.511	109.0	89.2	24
3	1.347	1.562	106.5	78.6	*b*

[a] CF_2 group. [b] Present study.

they are longer than those in perfluorocyclopropane (**17**; 1.314 Å)[22] and perfluorocyclobutane (**18**; 1.335 Å, 1.324 Å).[23,24] The endocyclic C−C bond length in **3** (1.562 Å) exceeds only slightly the 1.547 Å value found in the hydrogenated bicyclic cage of 1,3-diacetylbicyclo[1.1.1]pentane (**19**).[25] As a rule FCF angles are smaller than HCH angles in unfluorinated analogous compounds, and the C−CF_2−C angles larger than C−CH_2−C.[18] The 106.52° FCF angles in **3** are among the smallest known, presumably due to steric repulsion between proximate fluorines. The CCC angles in **3** and **19** also differ significantly, 84° at the bridgehead and 79° at the bridge in **3**, compared with 88° and 74°, respectively, in **19**. This is reflected in a greatly increased bridgehead-to-bridgehead separation, 1.979 Å in **3** as opposed to 1.875 Å in **19**.

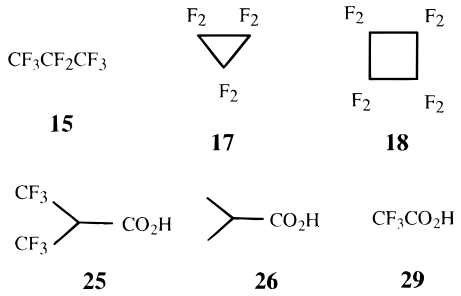

15 **17** **18**

25 **26** **29**

The structural effects of fluorination make sense in terms of Bent's rules.[26] The hybrids used in the CF bonds are enriched in p character compared to those used in CH bonds, and smaller FCF angles and larger CC(bridge)C angles in **3** compared to **19**, as well as the greatly increased interbridgehead distance, reflect increased s character in the carbon atomic hybrids used in CC bonds.

MP2/6-31G* calculations for **13** provide numerical support for this interpretation. Unconstrained optimization yielded a cage geometry very close to that observed for **3** (Figure 1), and a bridgehead-to-bridgehead distance of 1.967 Å [this level of calculations yields 1.874 Å for this distance in bicyclo[1.1.1]-pentane (**20**)[27]]. The most serious discrepancy between the geometry observed for **3** and that calculated for **13** is the distance between proximate fluorine atoms, computed to be almost 0.1 Å longer than observed in **3**. This is unlikely to be the result of the presence of two carboxymethyl groups in **3**, and probably results from the accumulation of small errors in the computed valence angles. It appears that MP2/6-31G* level of calculations overestimates the resistance put up by nonbonded fluorines when they are pushed together.

Analysis of the density matrices of **13** and **20** in terms of Weinhold's natural hybrid orbitals[28] yielded results collected in Table 2. It is seen that the exocyclic hybrid orbitals used by the bridge carbons indeed have much higher p character in **13** than in **20**, and the endocyclic ones have much higher s character, accounting for the difference in the valence angles. The negative atomic charges on the bridgehead carbons in **13** are remarkably large, almost twice those in **20** (Table 2). This suggests that fluorine lone pairs participate in σ-electron delocalization, and it is possible to write resonance structures with a double bond to fluorine and a negative charge on the bridgehead carbon. Since the CF bond is so short, the overlap of the fluorine lone pair orbitals with the p orbitals of the carbon neighbor is high, and formal donation of electron density from the former does not remove it from the highly electronegative fluorine atom much. Similar fluorine lone pair participation has been recently postulated in fluorocubane.[29] The calculated positive charge on the bridgehead hydrogen in **13** is also remarkably high.

We were unable to grow suitable crystals of **2** and have at our disposal only the MP2/6-31G* values for a model compound, 2,2,4,4,5-pentafluorobicyclo[1.1.1]pentane (**21**; Figure 3). They suggest that the substitution of one fluorine by hydrogen in the perfluorinated cage causes a certain amount of strain relief in that it permits the crowded geminal fluorines to move a little further apart (2.162 and 2.171 Å in **21**, compared to 2.155 Å in **13**). However, two of the proximate fluorine atoms, F(B) and F(E), actually move 0.015 Å closer to each other (distance **e** in Figure 3), presumably as a result of the HCF valence angle in **2** being a little larger (108.3°) than the FCF angles in **3** (106.5°). The computed distance between the hydrogen atom and the proximate fluorine four bonds away is 0.46 Å shorter than the sum of the atomic van der Waals radii. The calculated separation of the other two proximate fluorine atoms (distance **d** in Figure 3) is the same as in **13** (2.495 Å) and is 0.44 Å shorter than twice the fluorine van der Waals radius. It is likely that this value is subject to a similar error as was the case in **13**, and that the real distance in **2** is the same as in **3**, nearly 0.5 Å shorter than twice the van der Waals radius. The computed bridgehead-to-bridgehead distance in **21** is 0.014 Å shorter than in **13**.

Calculated Strain Energies of 13 and 21. The strain energies of **13** and **21**, *SE*(**13**) and *SE*(**21**), can be estimated from their calculated energies, *E*(**13**) and *E*(**21**), by comparison with the known calculated energy and strain energy of a similar compound.[30] We choose **20** as the reference, and take alkanes and fluorinated alkanes as standards, strain-free by definition. As shown in Scheme 3, the isodesmic reaction (1) of **20** with three molecules of **14** to yield **13** and three molecules of propane[31] (**22**) was calculated at the MP2 (RHF)/6-31G* level, including zero-point energy corrections, to be unfavorable by 33 (32) kcal/mol. An analogous reaction (2) of **20** with two molecules of **14** and one molecule of 2-fluoropropane (**23**), yielding **21** and three molecules of **22**, is unfavorable by 21 (20) kcal/mol. Adding to these energies the experimental strain energy of **20** (68 kcal/mol[8]), we estimated *SE* (**13**) to be 101

(21) Perretta, A. T.; Laurie, V. W. *J. Chem. Phys.* **1975**, *62*, 2469.
(22) Chiang, J. F.; Bernett, W. A. *Tetrahedron* **1971**, *27*, 975.
(23) Chang, C. H.; Porter, R. F.; Bauer, S. H. *J. Mol. Struct.* **1971**, *7*, 89.
(24) Alekseev, N. V.; Barzdain, P. P. *Zh. Strukt. Khim.* **1974**, *15*, 181.
(25) Friedli, A. C.; Lynch, V. M.; Kaszynski, P.; Michl, J. *Acta Crystallogr*. **1990**, *B46*, 377.
(26) Bent, H. A. *Chem. Rev.* **1961**, *61*, 275.
(27) (a) Wiberg, K. B.; Rosenberg, R. E.; Waddell, S. T. *J. Phys. Chem.* **1992**, *96*, 8293. (b) Barfield, M. *J. Am. Chem. Soc.* **1993**, *115*, 6916.
(28) Reed, A. E.; Curtiss, L. A.; Weinhold, F. *Chem. Rev.* **1988**, *88*, 899. *NBO 4.0*: Glendening, E. D.; Badenhoop, J. K.; Reed, A. E.; Carpenter, J. E.; Weinhold, F., Theoretical Chemistry Institute, University of Wisconsin, Madison, 1994.
(29) Della, E. W.; Head, N. J. *J. Org. Chem.* **1995**, *60*, 5303.
(30) (a) Wiberg, K. B. *Angew. Chem., Int. Ed. Engl.* **1986**, *25*, 312. (b) Schleyer, P. v. R.; Williams, J. E.; Blanchard, K. R. *J. Am. Chem. Soc.* **1970**, *92*, 2377.
(31) Olivella, S.; Sole, A.; McAdoo, D. J. *J. Am. Chem. Soc.* **1996**, *118*, 9368.

Table 2. Calculated[a] Atomic Charges and Fraction of s Character in NHOs

	charges				fraction (%) of s character		
atom	**13**	**20**	**21**	bond	**13**	**20**	**21**
C (bridgehead)	−0.374	−0.212	−0.354	CC	21.8	23.1	21.8, 22.4, 21.8[b]
				CH	34.0	30.1	33.4
C (bridge)	+0.871	−0.427	+0.867, +0.871, +0.256[c]	CC	27.7	23.3	28.1, 28.0, 24.5[b]
				CF	22.3		22.3, 21.5, 22.3, 21.7, 20.8[d]
				CH		26.6	30.0
H (bridgehead)	+0.268	+0.221	+0.261	CH	100	100	100
F (bridge)	−0.400		−0.400, −0.419, −0.403, −0.409, −0.409[e]	CF	32.4		32.8, 32.4, 32.5, 32.6, 31.5[d]
H (bridge)		+0.210	+0.233	CH		100	100

[a] NBO[28] MP2/6-31G* calculations at MP2/6-31G* optimized geometry. [b] Fraction of s character in hybrids used in bond to C(A), C(B), and C(C), respectively. [c] Charges at C(A), C(B), and C(C), respectively. [d] Fraction of s character in hybrids used in bonds to F(A), F(B), F(C), F(D), and F(E), respectively. [e] Charges at F(A), F(B), F(C), F(D), and F(E), respectively.

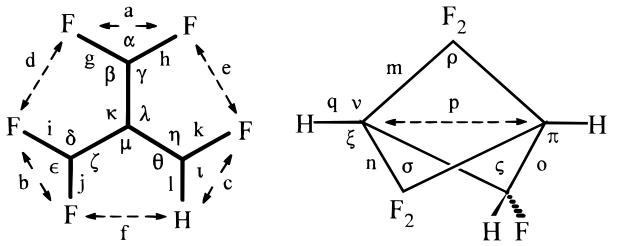

Distance	21	Distance	21	Angle	21	Angle	21
Å	Calcd	Å	Calcd	deg	Calcd	deg	Calcd
a	2.162	**j**	1.368	α	105.6	κ	84.7
b	1.272	**k**	1.373	β	118.2	λ	85.41
c	2.001	**l**	1.088	γ	117.7	μ	83.2
d	2.495	**m**	1.547	δ	119.8	ν	129.3
e	2.470	**n**	1.541	ϵ	105.9	ξ	128.9
f	2.232	**o**	1.559	ζ	116.4	π	129.1
g	1.359	**p**	1.954	η	118	ρ	78.3
h	1.355	**q**	1.090	θ	116.4	σ	78.7
i	1.353			ι	108.3	ς	77.6

Figure 3. Molecular geometry of **21** (calcd, MP2/6-31G*).

(100) kcal/mol and *SE*(**21**) to be 89 (88) kcal/mol. The origin of the additional strain may be seen in the naturally large C−CF_2−C valence angle, which causes the CF_2 group to resist incorporation into small rings [at the MP2 (RHF) level of calculation without inclusion of zero-point energies, **16** is 13.4 (13.6) kcal/mol more strained than cyclopropane].

The 13−16 kcal/mol difference between *SE*(**13**) and *SE*(**21**) provides a rough estimate of strain relief resulting from the substitution of one of the fluorine atoms in **13** by hydrogen. The existence of such relief was already deduced above from the inspection of the calculated geometries.

Calculated Gas-Phase Acidity of 13 and 21. The acidity of the bridgehead hydrogen will be important for many of the intended applications. An enthalpy for proton abstraction in **13** (ΔH_{acid}) was calculated to be 366.4 kcal/mol. Thus, in the gas phase **13** is expected to be about as strong an acid as CH_3-CN (ΔH_{acid} = 364.0 kcal/mol[32]). The analogous value for **20** was calculated to be 416.8 kcal/mol, and can be compared with

Scheme 3. Isodesmic Reactions for Estimation of Strain Energies

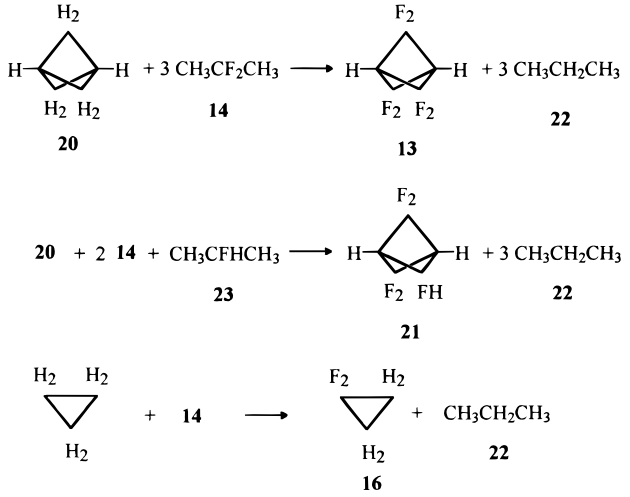

the observed[33] value of 411 ± 3.5 kcal/mol. For the bridgehead proton in **21**, ΔH_{acid} = 374.4 kcal/mol. Abstraction of the proton from the bridge carbon in **21** is more difficult, and the calculated enthalpy is 384.3 kcal/mol. This acid is about as strong as water (ΔH_{acid} = 384.1 kcal/mol[34]).

Acidity of 4 in Aqueous Solution. The pK_a values of **4** in water were measured by potentiometric titration to be 0.73 ± 0.15 and 1.34 ± 0.06, and can be compared to those measured for the parent diacid **24** (3.22 ± 0.02 and 4.26 ± 0.03). Thus, the introduction of the six fluorines lowers the first pK_a value by 2.55 pH units. This is surprisingly large compared with the 1.75 pH unit difference between 1,1,1,3,3,3-hexafluoroisobutyric (**25**; pK_a = 2.35)[35] and isobutyric (**26**; pK_a = 4.1)[36] acids. In order to reduce the uncertainty in the potentiometric determination of the first dissociation constant of **4**, we also attempted to measure the pK_a valuess for **4** and **24** by means of conductometry of their aqueous solutions.[37] Unfortunately, we were unable to obtain useful results since the concentrational dependence of conductance of solutions of both acids and their sodium salts could not be approximated by the Kohlrausch law

(32) Koppel, I. A.; Taft, R. W.; Anvia, F.; Zhu, S.-Z.; Hu, L.-Q.; Sung, K.-S.; DesMarteau, D. D.; Yagupolskii, L. V.; Yagupolskii, A. Yu.; Ignatev, N. V.; Kondratenko, N. V.; Volkonskii, A. Yu.; Vlasov, M. V.; Notario, R.; Maria, P.-C. *J. Am. Chem. Soc.* **1994**, *116*, 3047.

(33) Graul, S. T.; Squires, R. R. *J. Am. Chem. Soc.* **1990**, *112*, 2517.

(34) Lias, S. G.; Bartmess, J. E.; Liebman, J. F.; Holmes, J. L.; Levin, R. D.; Mallard, G. W. *J. Phys. Chem. Ref. Data* **1988**, *17*, Suppl. 1.

(35) England, D. C.; Krespan, C. G. *J. Am. Chem. Soc.* **1966**, *88*, 5582.

(36) *(36) Handbook of Chemistry and Physics*, 48th ed.; Weast, R. C., Selby, S. M., Eds.; The Chemical Rubber Co.: Cleveland, OH, 1968; p D-108.

(37) (a) Spiro, M. In *Physical Methods of Chemistry*, 2nd ed.; Rossiter, B. W., Hamilton, J. F., Eds.; John Wiley: New York; 1986; Vol. II, p 663. (b) Justice, J.-C. In *Comprehensive Treatise of Electrochemistry*; Conway, B. E., Bockris, J. O'M., Yeager, E., Eds; Plenum Press: New York; 1983; Vol. 5, p 223.

of independent ionic migration[37] and Fuoss−Onsager equation for concentration dependence of conductance.[37,38] The most probable reason for such behavior is multiple ion association in the solutions of these acids and salts even at low concentration.

Over the years the mechanism by which electronegative substituents increase the acidity of carboxylic acids has received much attention.[39] A general consensus seems to have been reached that direct field effect is much more important than the classical σ-inductive effect,[39a] even though substituent effect in some compounds is not straightforward to account for accurately by either one.[39b] In **4**, the six CF bond dipoles are oriented perpendicular to the 3-fold cage symmetry axis, and cancel each others' contribution to the electric field exactly at the center of the cage. Since this collection of charges provides no net dipole, we expected its electric field to fall off fast with distance, and the direct field effect of the six fluorine atoms on the pK_a value of **4** to be smaller than that of the six fluorines on the pK_a value of **25**, where the six CF bonds combine to produce a net dipole. The measured values thus came as a surprise and seemed to suggest a role for the σ-inductive effect.

However, when we evaluated the contribution of the direct field effect of fluorination on the acidity of the bicyclo[1.1.1]-pentane-1-carboxylic acid (**27**), **26**, and acetic acid by a numerical calculation of the electric field and electrostatic potential generated by a system of point charges located at the positions of carbons and fluorines of CF_3 and CF_2 groups in 2,2,4,4,5,5-hexafluorobicyclo[1.1.1]pentane-1-carboxylic acid (**28**), **25**, and trifluoroacetic acid (**29**), assuming a constant CF dipole, the initial expectation turned out to be wrong. For all three acids the electric field at the point where the carboxylic proton projects on the direction of the C−C bond holding the carboxylate group is very nearly equal. The electrostatic potential at this point is significantly lower for **25** than for **28** and **29**; the latter two are very close. At the exact location of the proton the potential in **29** is somewhat higher than that in **28** and much higher than that in **25**. The order of potentials matches the order of dissociation constants of the acids in aqueous solutions (pK_a for trifluoroacetic acid in aqueous solution is 0−0.2 as measured by different methods,[40] and for acetic acid, it is 4.75[36]), supporting the usual notion that the direct field effect of fluorine atoms is the major factor in the acidity increase. A much larger increase in acidity from acetic to trifluoroacetic acids compared with the increase from **24** to **4** is not explained this simply, and undoubtedly requires explicit consideration of the solvent and perhaps of hybridization changes as well.

In an attempt to separate the direct field effect of substitution of hydrogens for fluorines from a possible geometry change effect, we calculated the gas phase acidities of **28** and **27** at (RHF/6-31G*) optimized cage geometries of both. From the results shown in Scheme 4 we conclude that fluorination causes a larger change in acidity than does a geometry change. Still, geometry effects, presumably mediated by hybridization changes, are not negligible. For both compounds, the acidity is highest at their own optimized geometry. A reduction of the inter-bridgehead distance in **28** causes a significant decrease of acidity, and an elongation of the interbridgehead distance in **27** causes an even larger decrease of acidity. These data confirm that the acidity can change significantly with a geometrical distortion, but they do not allow us to separate unambiguously the part of the effect that is due to a geometrical change from other effects on the acidity of bicylo[1.1.1]pentanecarboxylic acids.

Scheme 4. Calculated Gas-Phase Acidities of **28** and **27** at Different Geometries

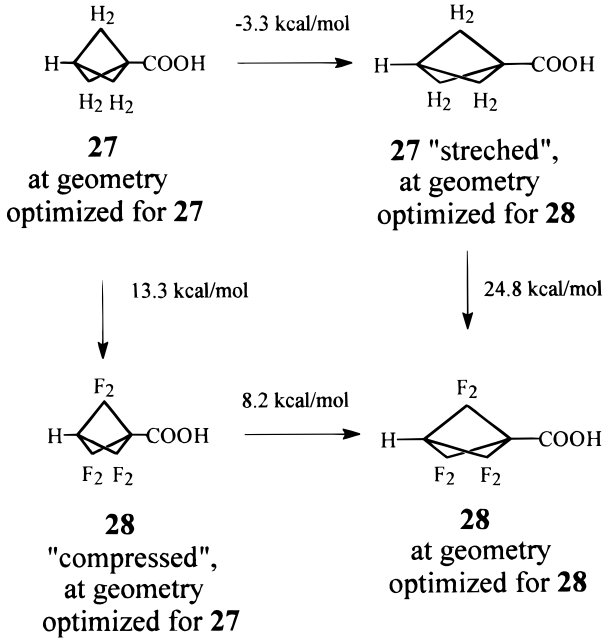

Table 3. NMR Chemical Shifts and Coupling Constants in **2**

		J (Hz)					
nucleus	δ (ppm)[a]	F(A)	F(B)	F(C)	F(D)	F(E)	H
F(A)	−95.96		+156.2	+70.6	+4.8	< 0.5	+22.6
F(B)	−115.90			+7.8	−11.4	+85.4	< 0.5
F(C)	−118.70				+162.0	−14.7	−1.4
F(D)	−128.68					< 0.5	+1.3
F(E)	−201.82						+62.7
H	5.88						
C(A)[b]	113.36	303	301	2	22	2	20
C(B)[b]	110.77	5	30	291	305	33	33
C(C)[b]	83.30	7	< 2	17	17	258	201
C[b,c]	65.58	19	19	19	19	19	< 2

[a] Ppm from $CFCl_3$, $CDCl_3$ (δ 77.0), or TMS. [b] For J_{CF} and J_{CH} signs were not determined. [c] Bridgehead.

Analysis of the NMR Spectra of 2. The spectra of the pentafluorinated diester **2** are first-order and are easier to analyze than the spectra of hexafluorinated diester **3**. The ^{19}F NMR of **2** exhibits five multiplets, and the ^1H NMR shows a doublet of doublets of triplets for the proton on the bicyclic cage.[15] The attribution of the short- and long-range coupling constants to the five fluorines F(A)−F(E) and the lone hydrogen was aided by $^{19}F\{^{13}C\}$ heteronuclear multiple-quantum coherence (HMQC)[41] experiments tuned to observe coupling constants of different magnitude (∼300, ∼30, and ∼15 Hz). The chemical shifts and coupling constants are collected in Table 3.

The largest J_{FF} coupling constants have values typical of geminal $^2J_{FF}$ ($J \simeq 160$ Hz) coupling and the largest J_{CF} coupling constants have values expected for one-bond $^1J_{CF}$ coupling ($J \simeq 300$ Hz). The nuclei F(A) and F(B) are very strongly coupled to C(A), nuclei F(C) and F(D) are coupled to C(B) with constants of comparable size, and F(E) couples strongly to C(C).

(38) Fuoss, R. M.; Onsager, L. *J. Phys. Chem.* **1957**, *61*, 668.

(39) For a general discussion see: (a) March, J. *Advanced Organic Chemistry*, 4th ed.; John Wiley: New York, 1992; pp 17−19, and pp 263−272 and references therein. (b) Exner, O.; Friedl, Z. *Prog. Phys. Org. Chem.* **1993**, *19*, 259. (c) Bowden, K.; Grubbs, E. J. *Prog. Phys. Org. Chem.*, **1993**, *19*, 183. (d) Bowden, K.; Grubbs, E. J. *Chem. Soc. Rev.* **1996**, *25*, 171.

(40) Milne, J. B.; Parker, T. J. *J. Solution Chem.* **1981**, *10*, 479 and references cited therein.

(41) Guide to NMR Experiments. VNMR 4.3; Varian, Nuclear Magnetic Resonance Instruments Pub. No. 87-195140-00, Rev. A0993.

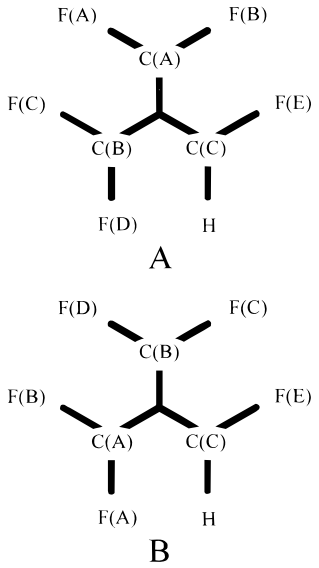

Figure 5. End-on view of the bicyclic cage of **2** and proposed NMR assignment.

We label the fluorine atoms such that F(A) is geminal with F(B), $J_{F(A)F(B)} = 156.2$ Hz, and both reside on C(A), and F(C) is geminal with F(D), $J_{F(C)F(D)} = 162.0$ Hz, and both reside on C(B). The fifth fluorine, F(E), is located on C(C), along with the lone hydrogen, $^2J_{F(E)H} = 62.7$ Hz, $^1J_{CH} = 201$ Hz.

All remaining coupling constants involving the fluorines and the hydrogen must be of the four-bond $^4J_{FF}$ and $^4J_{HF}$ types. The stereospecificity of the long-range $^4J_{FF}$ constants is striking. Two are extremely large, $J_{F(A)F(C)} = 70.6$ Hz, and $J_{F(B)F(E)} = 85.4$ Hz, and two are immeasurably small, $J_{F(A)F(E)}$ and $J_{F(D)F(E)}$ (<0.5 Hz). One of the $^4J_{HF}$ values is much larger than the others, $J_{HF(A)} = 22.6$ Hz, again demonstrating remarkable stereospecificity. Spin-tickling[42] $^{19}F\{^{19}F\}$ experiments were performed to determine the relative signs of J_{FF} and J_{HF} coupling constants. When the $^2J_{FF}$ values were presumed positive, like all other known coupling constants of this kind,[43] the absolute signs for all constants resulted. Three of them are negative.[15]

Table 3 also lists the coupling constants for the carbon atoms, and those involving the bridge carbons C(A), C(B), and C(C) are particularly informative. The $^2J_{CF}$ values are very similar for all the CF_2 fluorine nuclei in **2**, as is the case for majority of fluorocycloalkanes.[44] The two $^3J_{CH}$ and the $^3J_{CF}$ coupling constants are again very stereospecific and range from undetectable (<2 Hz) to very large (33 Hz). On the basis of HMQC spectra (Figure 4 in the Supporting Information), the $^3J_{CF}$ constants were divided into four groups: those close to 30 Hz [C(B)−F(B) and C(B)−F(E)], those between 30 and 15 Hz [C(A)−F(D)], those close to 15 Hz [C(C)−F(C) and C(C)−F(D)], and those much smaller than 15 Hz [C(A)−F(C), C(A)−F(E), C(B)−F(A), C(C)−F(A), C(C)−F(B)]. The final assignment was based on partially ^{19}F and ^1H decoupled ^{13}C NMR spectra.

Assignment of NMR Spectra of 2. While the identity of F(E) as the fluorine of the CHF bridge is obvious, those of the fluorines F(A)−F(D) are not (Figure 5; the molecule is viewed along the C1−C3 line). For full stereochemical assignment we need to determine (i) whether fluorine F(E) is located syn to carbon C(A) or carbon C(B), (ii) whether F(A) or F(B) is syn to C(C), and (iii) whether F(C) or F(D) is syn to C(C). Since no prior information on long-range J_{FF} and J_{HF} coupling constants in the highly strained fluorinated bicyclo[1.1.1]pentane cage is available, we cannot be absolutely sure from the values of the coupling constants alone which one of the eight possible assignments is correct.

We reduce the number of possibilities from eight to two by assuming that the unusually high values of the $J_{F(A)F(C)}$ and $J_{F(B)F(E)}$ coupling constants are both caused by the same special stereochemical relationship. Two such relationships come to mind: spatial proximity and a pseudo-W arrangement (the four bonds of the W's in **2** are not all in the same plane). In the former case ("proximity-dominated" J_{FF}), F(A), F(C) and F(B), F(E) are pairs of adjacent fluorine atoms that are pushed into uncomfortable nonbonded proximity (assignment in Figure 5a). In the latter case ("W-dominated" J_{FF}), these are the pairs of most distant fluorine atoms that are in an approximate W relationship (assignment in Figure 5b).

In either assignment the strikingly large $^4J_{F(A)H}$ constant is attributed to the nondominant stereochemical relationship. In the proximity-dominated case (Figure 5a), atoms F(A) and H are in a pseudo-W relation, and in the W-dominated case (Figure 5b), they are proximate. Clearly, whatever the correct assignment, the J_{HF} constant is large for a different stereochemical reason than the J_{FF} constant. Since the large long-range J_{HH} coupling constants usually are those that follow a W coupling path,[45] since J_{HH} and J_{HF} coupling constants often are roughly proportional,[46] and since the W coupling path is not particularly noted for producing large long-range J_{FF} coupling constants,[47] it would appear that the proximity-dominated case of Figure 5a is more likely. However, the strained cage system of **2** is sufficiently unusual that we hesitate to rule out the W-dominated case of Figure 5b.

Among the smaller $^4J_{FF}$ constants, $J_{F(C)F(E)}$ and $J_{F(B)F(D)}$ are distinctly larger than the others, perhaps with the exception of $J_{F(B)F(C)}$. This is sensible, in that in either assignment the F(C), F(E) and F(B), F(D) pairs of fluorines are in the nondominant but still special steric relationship, while the other pairs are neither in spatial proximity nor in a pseudo-W relationship. Indeed, among the latter, the origin of the small but still distinct difference between $J_{F(B)F(C)}$, on the one hand, and $J_{F(A)F(E)}$, $J_{F(D)F(E)}$, and to a lesser degree $J_{F(A)F(D)}$, on the other hand, must be attributed to secondary effects.

An additional weak argument in favor of the assignment shown in Figure 5a is suggested by consideration of the $^3J_{CF}$ coupling constants. For these, two steric relationships between the carbon and fluorine atoms are possible, one Z-shaped and one U-shaped. Although neither set of three bonds is planar, it appears more reasonable for the Z-shaped coupling path to provide the larger coupling constants. Inspection of Table 3 shows that this happens for the proximity-dominated assignment (Figure 5a), whereas in the W-dominated assignment (Figure 5b), the U-shaped path would generally provide the larger coupling constants.

In summary, although the above purely empirical reasoning suggests that the assignment shown in Figure 5a is more likely than that of Figure 5b, and singles out these two as most probable among the eight that are possible, some uncertainty remains. We have therefore sought help in quantum chemical calculations. The size of the molecules does not permit a

(42) Günther, H. *NMR Spectroscopy. An Introduction*; John Wiley and Sons: New York, 1980; p 292.

(43) See ref 42, p 351.

(44) Schneider, H.-J.; Gschwendtner, W.; Heiske, D.; Hoppen, V.; Thomas, F. *Tetrahedron* **1977**, *33*, 1769.

(45) (a) Jackman, L. M.; Sternhell, S. *Application of Nuclear Magnetic Resonance Spectroscopy in Organic Chemistry*, 2nd ed.; Pergamon Press: Oxford; p 334. (b) Wiberg, K. B.; Lowry, B. R.; Nist, B. J. *J. Am. Chem. Soc.* **1962**, *84*, 1594. (c) Wiberg, K. B.; Lampman, G. M.; Ciula, R. P.; Connor, D. S.; Schertler, P.; Lavanish, J. *Tetrahedron* **1965**, *21*, 2749.

(46) Middleton, W. J.; Lindsey, R. V. *J. Am. Chem. Soc.* **1964**, *86*, 4948.

(47) Hirao, K.; Nakatsuji, H.; Kato, H. *J. Am. Chem. Soc.* **1972**, *94*, 4078.

Table 4. NMR Chemical Shifts in **2** and **21**

nucleus[a]	**21** (calcd[b]) $-\Delta\sigma^c$ (ppm) rel to **3**	**2** (obsd) $\Delta\delta^d$ (ppm) rel to **13**	nucleus[a]	**21** (calcd[b]) $-\Delta\sigma^c$ (ppm) rel to **3**	**2** (obsd) $\Delta\delta^d$ (ppm) rel to **13**
F(A)	19.49	20.26	C(A)	4.06	3.10
F(B)	−0.04	0.26	C(B)	0.91	0.51
F(C)	−3.77	−2.54	C(C)	−28.16	−26.94
F(D)	−15.70	−12.52	C[e]	−3.64	−3.21
F(E)	−81.16	−85.66			

[a] See Figure 5a for atom labels. [b] GIAO-SCF/6-31G*, at MP2/6-31G* optimized geometries (Figure 3). For details see the text. [c] Relative NMR chemical shifts were obtained as minus the relative NMR chemical shieldings. NMR chemical shielding computed for nuclei in **21** relative to those computed for nuclei in **13**, $\sigma(F) = 352.56$ ppm, $\sigma(C_{bridge}) = 143.01$ ppm, $\sigma(C_{bridgehead}) = 99.91$ ppm. [d] NMR chemical shifts observed for nuclei in **2** relative to those observed for **3**, $\delta(F) = -116.16$ ppm, $\delta(C_{bridge}) = 110.26$ ppm, $\delta(C_{bridgehead}) = 68.79$ ppm. [e] Bridgehead.

reliable computation of the spin−spin coupling constants, given our present resources. Although for a molecule of the size of **2** only very crude calculations of chemical shifts are possible today with programs that are easily available, we believe that the simpler model molecules **13** and **20** will show the same trends. Still, the presence of five carbons and five or six fluorines prevents us from using a large basis set with a correlated wave function, and the calculated chemical shifts can only be expected to agree semiquantitatively. Since the observed shifts of C(A) and C(B) differ by less than 3 ppm and are both nearly identical to the value observed for the CF_2 carbons in **3** (110.26 ppm), the calculation will not be able to distinguish between these two carbons reliably.

Fortunately, the observed chemical shift of F(A) is about 20.3 ppm less negative than those of F(B) and F(C), which are nearly equal to those of the fluorines in **3** (−116.16 ppm), whereas that of F(D) is about 12.5 ppm more negative. These differences are quite striking, particularly that between the chemical shifts of F(A) and F(B), which only differ in their stereochemical relation to a rather distant hydrogen on another bridge. There apparently is efficient electronic communication across the strained cage. Although most of the past computational experience pertains to ^{13}C chemical shifts,[48] it still suggests that these large ^{19}F chemical shift differences should be reproduced even at the 6-31G* Hartree−Fock level (at an MP2/6-31G* optimized geometry) that is feasible for us today.

In the two assignments considered most likely (Figure 5), one of these two special fluorines in **2** is in a pseudo-W relation to the proton, and the other is spatially proximate to the proton. As shown in Table 4, the calculations predict that relative to the chemical shift of the fluorines in **13**, that of the fluorine in the pseudo-W relation to the proton in **13** is about 19.5 ppm less negative, and that of the fluorine that is spatially proximate to the proton in **13** is about 15.7 ppm more negative. Assuming that the presence of the carbomethoxy groups in **2** and **3** has only a minor effect on the chemical shift differences in the pentafluorinated and the hexafluorinated cage, these results identify the assignment in Figure 5a as correct.

Analysis and Assignment of NMR Spectra of 3. The ^{13}C NMR spectrum of the diester **3** shows a multiplet of more than 100 lines attributed to a bridge carbon (Figure 6a). The absence of symmetry suggests that the $^{13}CF_2$ and $^{12}CF_2$ fluorines are inequivalent. The spectrum was simulated as an AXX′-YY′Y″Y‴ spin system, starting with averages of the corresponding coupling constants obtained above for **2**. Iteration yielded a match for the observed spectrum (Figure 6a). Several simulation attempts starting with coupling constant values

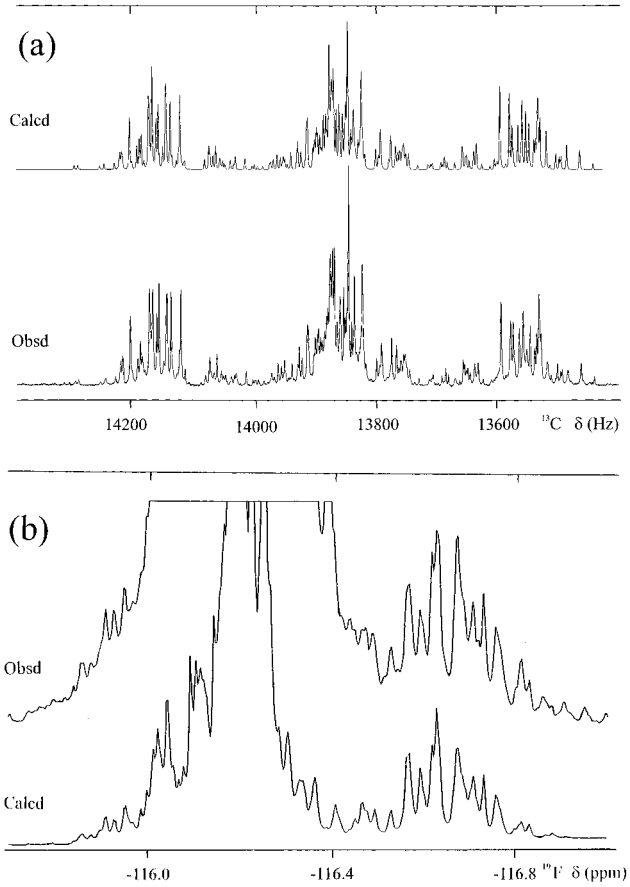

Figure 6. Observed and simulated undecoupled spectra of **3**: (a) ^{13}C and (b) ^{19}F (^{13}C satellites).

modified by 10 Hz converged to the same result. An iteration starting with interchanged values of constants $^4J_{FF}$ across the W-shaped and U-shaped paths failed to converge to a fit to the observed spectrum.

The initial set of parameters treated the coupling constants of the fluorine nuclei in $^{13}CF_2$ as equal to those in $^{12}CF_2$, even though their chemical shifts differ. Subsequently, this symmetry constraint was removed, and further iteration yielded somewhat different coupling constant values for the two types of fluorines (Table 5). The slight difference between the coupling constants involving $^{13}CF_2$ and $^{12}CF_2$ fluorine atoms (up to 0.3 Hz) exceeds the statistical error margins (0.03 Hz with 90% confidence) of the iteration procedure, but not by much. If it is real, it represents a rare example of a third-atom isotopic effect on coupling constants.

In order to obtain an independent verification of the correctness of the coupling constants derived from the simulation program, the coupling constants and the isotopic shift of the ^{19}F nuclei derived from the ^{13}C NMR spectrum (Figure 6a, Table 5) were used without any adjustment to simulate the ^{13}C

(48) (a) Chesnut, D. B. *Annu. Reports NMR Spectrosc.* **1994**, *29*, 71. (b) Kutzelnigg, W.; van Wüllen, Ch.; Fleischer, U.; Franke, R.; Mourik, T. V. In *NMR Shieldings and Molecular Structure*; Tossel, J. A., Ed.; Kluwer Academic Publishers: Norwell, MA, 1993; pp 141−161. (c) Facelli, J. C.; Grant, D. M.; Michl, J. *Acc. Chem. Res.* **1987**, *20*, 152. (d) Siehl, H.-U.; Müller, T.; Gauss, J.; Buzek, P.; Schleyer, P. V. R. *J. Am. Chem. Soc.* **1994**, *116*, 6384.

Table 5. Spin-Spin Coupling Constants in **3**

coupling constant type	coupling constant[a] (Hz)	coupling constant type	coupling constant[a] (Hz)
$^1J_{CF}$	−299.3	$^4J_{FF}$ (proximate fluorines)	97.9[c]
$^2J_{FF}$	160.6[b]		97.6[d]
	160.4[c]	$^4J_{FF}$ (sickle-shaped path)	8.6
$^3J_{CF}$ (Z-shaped path)	25.1	$^4J_{FF}$ (W-shaped path)	−10.3[c]
$^3J_{CF}$ (U-shaped path)	−4.0		−10.2[d]

[a] Coupling constants were calculated within 0.03 Hz limits with 90% confidence. [b] Both ^{19}F atoms bound to ^{13}C. [c] Both ^{19}F atoms bound to ^{12}C. [d] One ^{19}F atom bound to ^{12}C, the other bound to ^{13}C.

satellites in the ^{19}F spectrum (Figure 6b). In spite of a relatively low signal-to-noise ratio in the satellite spectrum, the agreement with the simulated spectrum is most satisfactory. The signals of the ^{13}C satellites partially overlap with a very strong singlet that is due to the $^{12}CF_2$ fluorines. The ^{13}C isotopic effect on the ^{19}F chemical shift is particularly clear from the displacement of this strong singlet from the center of the ^{13}C satellite pattern.

The coupling constants derived for **3** follow the same trends as those obtained for **2**: the constant $^4J_{FF}$ between proximate fluorines is huge, 98 Hz, the $^4J_{FF}$ constant across the W-shaped path is negative and a little larger in absolute value than the positive $^4J_{FF}$ constant across the sickle-shaped path, and the $^3J_{CF}$ constant across the Z-shaped path is significantly larger than the one across the U-shaped path. This agreement can be considered as yet another piece of evidence in favor of the assignment of the NMR spectrum of **2** described above and shown in Figure 5a.

Spin−Spin Coupling Constants and Chemical Shifts in 2 and 3.[49] It is of interest to compare NMR characteristics of fluorinated bicyclo[1.1.1]pentanes with those of previously studied fluorinated hydrocarbons.

One-bond coupling constants $^1J_{CF}$ in **2** and **3** are similar to those in fluorocycloalkanes.[49] The $^1J_{CH}$ coupling constant is larger in **2** (201 Hz) than in parent bicyclo[1.1.1]pentanes (167 Hz),[45] in accord with the increased s character of the carbon hybrid orbital used in the CH bond (Table 2).

Geminal C−F coupling constants $^2J_{CF}$ in fluoroalkanes are known to depend primarily on the electronegativity and orientation of substituents on the carbon with respect to the coupled fluorine. The constants range from −11.3 Hz in fluoroethane[50] to 46 Hz (sign unknown) in perfluoroethane.[51] Since the methyl carboxylate substituents in **2** are oriented in the same way towards all the fluorines, it is no surprise that the $^2J_{CF}$ values do not differ. The 19 Hz value is close to those measured for other bicyclic fluorocarbons,[52] and it is noticeably smaller than those in 4-fluorocubane derivatives (24−25 Hz).[29]

Vicinal C−F coupling constants $^3J_{CF}$ in alicyclic compounds are stereospecific and follow a Karplus-type rule, $^3J_{CF} = 11.0 \cos^2 \theta$[44,52c] ($\theta$ is the FCCC dihedral angle). In bridgehead fluorinated adamantanes and diamantanes,[52a−c] $^3J_{CF}$ values range from −10.9 to +17.0 Hz. In 4-substituted bicyclo[2.2.2]oct-1-yl fluorides,[52d] $^3J_{CF}$ constants are 7.9−11.3 Hz, and in 4-substituted fluorocubanes they are even smaller, 4−7 Hz.[29] The largest $^3J_{CF}$ value reported is 42.5 Hz in 1-fluorobicyclo-[1.1.1]pentane.[52d] In **2** and **3**, the $^3J_{CF}$ values range from −4 to +25 Hz. These constants are stereospecific and follow the Karplus rule, but the largest values exceed those calculated from the above formula. Two constants observed in **2** differ significantly from the calculated values: $^3J_{C(C)F(A)}$ is unexpectedly small, and $^3J_{C(C)F(D)}$ is unexpectedly large.

The large $^3J_{CH}$ constants in **2**, in which the HCCC dihedral angles are close to either 0 or 180°, follow the Karplus-type rule for CH coupling constants[53] well.

The long-range couplings between proximate fluorines are among the largest known between aliphatic fluorines; cf. $^5J_{FF} = 75$ Hz between two of the fluorines in bis(trifluoromethyl)-tetrachloroethane (at −150 °C),[54] $^5J_{FF} = 105$ Hz between fluorines in an aziridine derivative of the *endo* dimer of perfluorocyclopentadiene,[55] and $^4J_{FF} = 78$ and 81 Hz in 1,2,3-trichlorononafluoronorbornane.[56] The large magnitudes of these coupling constants in **2** and **3** are undoubtedly due to the very short distance between the nonbonded fluorines, about 0.5 Å shorter than the van der Waals radii. An even much larger value, 170 Hz, has been reported for $^5J_{FF}$ between aromatic fluorines in a 1-substituted 4,5-difluoro-8-methylphenanthrene.[57]

The $^4J_{FF}$ constants are perhaps the least well understood. Those across the W-shaped paths in **2** and **3** are smaller and negative. Their absolute values are only a little larger than those of the positive $^4J_{FF}$ constants across sickle-shaped paths in **3** and in half of the cases in **2**. Surprisingly, F(E) does not couple detectably with F(A) and F(D) across the sickle-shaped path. Similar constants in adamantanes and diamantanes fluorinated on bridgeheads were reported to range from ±2.5 Hz for the latter to +10 Hz for the former.[49] In fluorinated acyclic allylic cations the $^4J_{FF}$ constants decrease in absolute magnitude in the order "U" > "W" > "sickle", without changing sign.[58]

The $^4J_{HF}$ coupling constant across the W-shaped path in **2**, $J_{HF(A)} = 22.6$ Hz, is undoubtedly one of the largest known long-range hydrogen−fluorine coupling constants. The record holder probably is the bridgehead−bridgehead coupling constant along a W path in 1-fluorobicyclo[1.1.1]pentane,[59] $^4J_{HF} = 70.6$ Hz. Most of the examples of large $^4J_{HF}$ values occur across rings, such as 10.2 and 11.9 Hz in 3,3,4-trifluoro-4-chlorocyclobutane[60] (between the two nonequivalent fluorines of the CF_2 group and the diagonally opposed olefinic protons), and 11.6 Hz in 1,1,2-trifluoro-3-chlorocyclobutane[61] (between the fluorine and one of the diagonally disposed protons).

The $^4J_{HF}$ coupling between proximate H and F(D) is only 1.3 Hz. Although short in absolute terms, the H−F distance

(49) For compilations of coupling constants see: (a) Wray, V. *J. Chem. Soc., Perkin Trans. 2* **1976**, 1598. (b) Emsley, J. W.; Phillips, L.; Wray, V. *Prog. Nucl. Magn. Reson. Spectrosc.* **1975**, *10*, 83.
(50) Jensen, H.; Schaumburg, K. *Mol. Phys.* **1971**, *22*, 1041.
(51) Graves, R. E.; Newmark, R. A. *J. Chem. Phys.* **1967**, *47*, 3681.
(52) (a) Olah, G. A.; Shih, J. G.; Krishnamurthy, V. V.; Singh, B. P. *J. Am. Chem. Soc.* **1984**, *106*, 4492. (b) Krishnamurthy, V. V.; Shih, J. G.; Singh, B. P.; Olah, G. A. *J. Org. Chem.* **1986**, *51*, 1354. (c) Duddeck, H.; Islam, Md. R. *Tetrahedron* **1981**, *37*, 1193. (d) Della, E. W.; Cotsaris, E.; Hine, P. T. *J. Am. Chem. Soc.* **1981**, *103*, 4131. (e) Grutzner, J. B.; Jautelat, M.; Dence, J. B.; Smith, R. A.; Roberts, J. D. *J. Am. Chem. Soc.* **1970**, *92*, 7107.
(53) Karplus, M. *J. Chem. Phys.* **1959**, *30*, 11.
(54) Weigert, F. J.; Roberts, J. D. *J. Am. Chem. Soc.* **1968**, *90*, 3577.
(55) Banks, R. E.; Bridge, M.; Fields, R.; Haszeldine, R. N. *J. Chem. Soc. C* **1971**, 1282.
(56) Lindon, J. C. Ph.D. Dissertation, University of Birmingham, 1969, quoted in ref 49.
(57) Servis, K. L.; Fang, K.-N. *J. Am. Chem. Soc.* **1968**, *90*, 6712.
(58) Bakhmutov, V. I.; Galakhov, M. V.; Raevskii, N. I. *Izv. Akad. Nauk SSSR, Ser. Khim.* **1987**, 1884.
(59) Barfield, M.; Della, E. W.; Pigou, P. E.; Walter, S. R. *J. Am. Chem. Soc.* **1982**, *104*, 3549.
(60) Newmark, R. A.; Apai, G. R.; Michael, R. O. *J. Magn. Reson.* **1969**, *1*, 418.
(61) Park, J. D.; Michael, R. O.; Newmark, R. A. *J. Org. Chem.* **1964**, *29*, 3664.

(2.232 Å, MP2/6-31G*) is apparently still too large for the mechanisms of through-space spin−spin coupling[47,62] to operate, or else through-space and through-bond contributions cancel.

Conclusions

The bicyclo[1.1.1]pentane cage with penta- or hexafluorinated bridges is extremely highly strained. It features very closely spaced nonbonded fluorines and an increased bridgehead-to-bridgehead separation relative to the parent cage. It is susceptible to reductive C−C bond cleavage, exibits remarkable stereospecific NMR coupling constants and ^{19}F chemical shifts, and has a peculiarly large acidifying effect on a bridgehead carboxyl, apparently due to a direct field effect of the fluorine substituents.

Experimental Section

General Procedures and Characterization. Melting points were determined on a Boetius PHMK05 apparatus with a microscope attachment (4 °C/min). ^{19}F NMR spectra were obtained at 282.4 and 376.5 MHz on Varian VXR 300 and Bruker 400 spectrometers, respectively. ^{13}C NMR spectra were obtained at 100.6 and 125.7 MHz on Bruker 400 and Varian VXR 500 spectrometers, respectively. The former was used to obtain the ^{1}H spectrum at 400 MHz. HMQC ^{19}F-{^{13}C} experiments were done on a Varian VXR 500 spectrometer. The measurements were performed in chloroform-*d* solvent unless specified otherwise. Fluorotrichloromethane, chloroform-*d*, and tetramethylsilane internal standards were used for ^{19}F, ^{13}C, and ^{1}H NMR spectra, respectively, unless specified otherwise. Positive shifts are downfield. Infrared spectra were recorded on a Nicolet 800 FTIR instrument in CS_2 (**2** and **3**) or in KBr pellets (**4**, **5**, and **6**). Electron-impact mass spectra were taken on a HP 5988A GC−MS instrument. High-resolution mass spectra were taken on a VG 7070EQ instrument. Elemental analysis was performed by Desert Analytics, Tucson, AZ. Preparative GC was done on a SE-30 (20% on Chromosorb W) 6 ft long 1/4 in. diameter column.

Reagents. Commercially available samarium diiodide solution in THF (Strem), bromine (Fluka), mercury(II) oxide (Aldrich), and 1,2-dibromotetrafluoroethane (Aldrich) were used without purification.

Calculations. Computations were done on an IBM RISC 6000-590 workstation. All geometries were optimized at both RHF and MP2 levels of theory (except for **28**, **27**, and their conjugate carboxylate anions, whose geometries were optimized at the RHF level only) using the 6-31G* basis set for neutral molecules and 6-31+G* basis set for anions, with the GAUSSIAN 92 and GAUSSIAN 94 programs.[63] For the geometries optimized at RHF level vibrational frequency analysis was performed, and no imaginary frequencies were found. Enthalpies of proton abstraction were calculated at the MP2 (**13**, **20**, and **21**) and HF (**28** and **27**) level of theory, using the 6-31+G* basis set for both neutral and anionic forms, without zero-point corrections. Strain energies were calculated from isodesmic reactions with the 6-31G* basis set at the HF and the MP2 levels, with HF zero-point energy corrections. NMR chemical shifts were calculated using both the 6-31G and the 6-31G* basis sets with the ACES2[64] program at the GIAO−HF level for MP2/6-31G* optimized geometries. NMR simulations and iterations were performed with the PERCH 1/95[65] program on a 486/40 MHZ/8 Mb RAM IBM-compatible PC, and the Varian 4.3b[41] software on a SUN workstation. Nonlinear regression analysis of titration curves was performed with Axum 4.0 software.[66]

X-ray Diffraction on 3.[15] Crystals of **3** were grown from heptane solution in the form of clear, colorless parallelepipeds. Indexing was determined after collection of three sets of twenty 0.3° ω scans on a Siemens SMART CCD diffractometer with a graphite crystal monochromator using Mo Kα radiation. A least-squares refinement of final cell dimensions was performed using 5632 reflections. A hemisphere of data was collected. Equivalent reflections were merged and all data were corrected for Lorentz and polarization effects. No merging was performed on Friedel opposites. Structure solution by direct methods in the noncentrosymmetric space group $P2_12_12_1$ with dimensions a = 8.6131(10) Å, b = 9.8943(10) Å, and c = 12.4533(14) Å revealed the complete non-hydrogen structure. The final residuals were R = 2.54% [2446$I \geq 2\sigma(I)$] and wR = 6.97% (all data) for 186 parameters. The data were processed with the SHELXTL program[67] on a Silicon Graphics Indigo2 XL workstation.

X-ray Diffraction on Hydrolyzed 11.[15] Crystals were grown from water solution in the form of clear, colorless parallelepipeds. The crystal was selected under Exxon Paratone N oil and mounted in the 123 K N_2 cold stream of a Siemens LT-2A low-temperature apparatus attached to the Siemens SMART diffractometer using Mo Kα radiation. Initial cell parameters were determined from analysis of 3 sets of 20 detector frames. The orientation matrix was passed to SAINT[68] for integration of the intensity data. Cell parameters were refined after every 40 frames and final dimensions determined by utilizing all 3569 reflections with $I > 10\sigma(I)$.

Structure solution in monoclinic space group $P2_1/c$ revealed the non-hydrogen structure. Hydrogens were added at calculated positions which were allowed to ride on the position of the parent atom through the refinement. All non-hydrogen atoms were modeled with anisotropic parameters for thermal motion. Isotropic thermal parameters set to 1.2 times the equivalent isotropic thermal parameter of the parent atom were employed for hydrogen atoms. No unusual intermolecular contacts were noted.

Dimethyl Hexafluorobicyclo[1.1.1]pentane-1,3-dicarboxylate (3). A general procedure for direct fluorination[11] was followed. A 600 mL jacketed aluminum reactor equipped with a 50 cm double tube condenser set at −14 °C (described in detail elsewhere[11b]) was charged with $CF_2ClCFCl_2$ (400 mL), and a gas flow of F_2 (66 mL/min) and N_2 (244 mL/min) was begun. **Caution:** *Pure fluorine is extremely hazardous. All construction materials must be carefully passivated with diluted fluorine, and the reactor and fluorine supply must be barricaded.* The reactor temperature was set at 17 °C, and 210 mL of a solution of **7**[10] (11.0 g) in $CF_2ClCFCl_2$ was introduced by a syringe pump over a period of 4 h with vigorous stirring. The reactor was then purged with nitrogen for 1 h, the contents were mixed with 13% BF_3 in methanol (50 mL), and the solvent was distilled to leave a semisolid (8.0 g). At this point, GC−MS analysis showed that the major constituents were **2** (30%) and **3** (43%). The mixture was resubmitted to the fluorination and workup procedure described above. The distillation residue was crystallized from hexane to yield 6.3 g of an 88:12 mixture of **3** and **2** (by GLC). For most further use, **3** was further purified by crystallization from aqueous methanol, and the typical overall yield of material suitable for further work was about 40% based on **7**. An analytical sample was crystallized from a pentane−ether mixture (5:1): mp 73 °C; ^{1}H NMR δ 3.92; ^{13}C{^{1}H} NMR δ 53.54, 68.79 (septet, J = 19 Hz), 110.3 (br m), 156.45; ^{13}C-{^{19}F} NMR δ 53.54 (q, J = 15.0 Hz), 68.79, 110.26, 156.44 (q, J = 3.8 Hz); ^{19}F NMR (CCl_3F) δ −116.16; IR 1756 (C═O), 1331 (C−O), 1232 (C−F) cm^{-1}; EIMS, m/z 261 [M − MeO]$^+$ (1), 234 [M −

(62) Wasylishen, R. E.; Barfield, M. *J. Am. Chem. Soc*. **1975**, *97*, 4545.

(63) Frisch, M. J.; Trucks, G. W.; Head-Gordon, M.; Gill, P. M. W.; Wong, M. W.; Foresman, J. B.; Johnson, B. G.; Schlegel, H. B.; Robb, M. A.; Replogle, E. S.; Gomperts, R.; Andres, J. L.; Raghavachari, K.; Binkley, J. S.; Gonzalez, C.; Martin, R. L.; Fox, D. J.; Defrees, D. J.; Baker, J.; Stewart, J. J. P.; Pople, J. A. *Gaussian 92*, Revision C; Gaussian, Inc.: Pittsburgh, PA, 1992.

(64) (a) Stanton, J. F.; Gauss, J.; Watts, J. D.; Lauderdale, W. J.; Bartlett, R. J. *ACES II. Quantum Theory Project*; University of Florida: Gainsville, FL, 1991. ACES II includes the VMOL integral and VPROPS property integral programs of J. Almlöf and P. R. Taylor and a modified version of the integral derivative program ABACUS written by T. Helgaker, H. J. Aa. Jensen, P. Jørgensen, J. Olsen, and P. R. Taylor. (b) Stanton, J. F.; Gauss, J.; Watts, J. D.; Lauderdale, W. J.; Bartlett, R. J. *Int. J. Quantum Chem. Symp.* **1992**, *26*, 879.

(65) Laatikainen, R.; Niemitz, M.; Sundelin, J.; Hassinen, T. *An Integrated Software for Analysis of NMR Spectra on PC*; Version 1/95, PERCH Project, University of Kuopio: Kuopio, Finland.

(66) *Axum 4.0 for Windows*; Copyright 1995, TriMetrix, Inc.

(67) Sheldrick, G. M. *SHELXTL. A Program for Crystal Structure Determination*, Version 5 beta; Siemens Analytical X-ray Instruments: Madison, WI, 1995.

(68) SAINT, v.4.036; Siemens Industrial Automation, Inc., Madison, WI, 1995.

COOMe]$^+$ (5), 171 (23), 93 (35), 81 (92), 59 (100). Anal. Calcd for $C_9H_6F_6O_4$: C, 37.00; H, 2.01; F, 39.02. Found: C, 37.05; H, 1.97; F, 38.60.

Dimethyl Pentafluorobicyclo[1.1.1]pentane-1,3-dicarboxylate (2). A small amount of this material was isolated from the above direct fluorination mixture by preparative gas chromatography: mp 41.5 °C; ^{1}H NMR and ^{19}F NMR (Table 1; CH_3 δ 3.87); ^{13}C{^{19}F} NMR (Table 2; CH_3 δ 53.34, COO δ 158.42, bridgehead C (one of the ^{19}F atoms decoupled) δ 65.58 (p, J = 19 Hz); IR 2952 (C−H), 1754 (C═O), 1328 (C−O), 1237 and 1198 (C−F) cm^{-1}; EIMS, *m*/*z* 243 [M − MeO]$^+$ (2), 214 (8), 153 (16), 106 (18), 93 (25), 81 (70), 75 (30), 63 (50), 59 (100). Anal. Calcd for $C_9H_7F_5O_4$: C, 39.43; H, 2.58; F, 34.65. Found: C, 39.34; H, 2.37; F, 34.76.

Hexafluorobicyclo[1.1.1]pentane-1,3-dicarboxylic Acid (4). A 50% aqueous solution of NaOH (1.280 g, 16 mmol) was added to a solution of **3** (2.0 g, 6.85 mmol) in methanol (20 mL). The reaction mixture was stirred for 1 h at room temperature and then was acidified with 37% aqueous HCl (3 mL). Solvents were removed on a rotary evaporator. A solid residue was extracted with acetone (two 10 mL portions). Upon evaporation of the solvent, the combined extracts yielded 1.652 g (91% yield) of the diacid. An analytical sample was sublimed (10^{-5} Torr, 70 °C): mp 206−208 °C (dec); ^{13}C{^{19}F} NMR (acetone-d_6) δ 70.03, 111.44, 157.34; ^{19}F NMR (acetone-d_6) δ −116.76; IR 3408 (O−H), 1731 (C═O), 1414 (C−O), 1224 (C−F) cm^{-1}; EIMS, *m*/*z* 236 [M − CO]$^+$ (11), 218 [M − CO_2]$^+$ (32), 200 (35), 183 (33), 174 (57), 159 (100), 137 (54), 124 (69), 93 (69), 69 (79), 44 (100); CIMS (NH_3), *m*/*z* 280 [M + NH_4]$^+$.

1,3-Dibromohexafluorobicyclo[1.1.1]pentane (5). A mixture of **4** (0.528 g, 2 mmol), mercury(II) oxide (1.0 g, 4.6 mmol), magnesium sulfate (0.4 g), and bromine (0.940 g, 5.9 mmol) in 1,2-dibromotetrafluoroethane was irradiated with a 150 W tungsten bulb for 36 h. Excess bromine and the solvent were distilled off, and a residue was sublimed (0.01 Torr, room temperature): yield 460 mg (68%); mp 77−78 °C; ^{13}C NMR δ 49.01 (septet, J = 21 Hz), 108.8 (br m); ^{13}C{^{19}F} NMR δ 49.01, 108.81; ^{19}F NMR (CCl_3F) δ −122.72 (s); IR (gas phase) 1292, 1259 (C−F), 1233, 874, 660, 643 cm^{-1}; EIMS, *m*/*z* 255 [M − Br] (100), 253 [M − Br] (94), 236 (21), 234 (23), 193 (54), 191 (50), 174 (14), 155 (30), 124 (92), 93 (58), 74 (33); HRMS *m*/*z* (calcd for $C_5{}^{79}Br^{81}BrF_6$ 333.8251) 333.8268.

1,3-Diiodohexafluorobicyclo[1.1.1]pentane (6). A 0.1 M solution of SmI_2 in THF (8.5 mL) was slowly added to a solution of **5** (0.285 g, 0.84 mmol) in THF (10 mL) at −78 °C. Aliquotes of the reaction mixture were taken for ^{19}F NMR[69] and GC−MS analysis during the addition of SmI_2 solution. As more SmI_2 was added, the intensity of the ^{19}F NMR signal at δ −122.8 ppm, attributed to **5**, decreased. The intensity of the signal at δ −121.5 ppm, due to **8**, judging by its mass spectrum,[70] increased in the beginning but decreased later, and the intensity of the signal at δ −120.2 ppm, attributed to **6**, increased.[71] After the reaction mixture turned yellow, it was distilled on a vacuum line with three traps at −40, −78, and −193 °C. A fraction collected at −40 °C was crystallized from pentane to give 0.112 g (31% yield) of a crude product containing 92% (^{19}F NMR) of **6**. An analytical sample was obtained by recrystallization from pentane: mp 25 °C; ^{13}C-{^{19}F} NMR δ 16.92, 107.86; ^{19}F NMR (CCl_3F) δ −120.34; IR (neat liquid) 1278, 1226 (C−F), 857, 641, 600 cm^{-1}; EIMS, *m*/*z* 428 [M] (16), 301 (100), 282 (29), 239 (10), 174 (51), 127 (29), 124 (69), 105 (10), 93 (14), 74 (17); HRMS *m*/*z* (calcd for $C_5F_6I_2$ 427.7994) 427.8001.

Sodium Hexafluorobicyclo[1.1.1]pentane-1,3-dicarboxylate (10). A suspension of **3** (0.52 g, 1.78 mmol) in a solution of NaOH (0.15 g, 3.7 mmol) in water (3 mL) was refluxed for 1.5 h. Water was evaporated under reduced pressure. The yield was 0.52 g (97%).

Reduction of 10. Sodium (0.240 g, 10.4 mol) was added in 60 mg pieces to a suspension of **10** (0.41 g, 1.37 mmol) in NH_3 (30 mL) over a period of 9 h. Ammonia was allowed to evaporate. The remaining solid was treated with aqueous HCl (35%, 1.1 mL) and extracted with ether (3 × 30 mL). The ethereal solution was treated with diazomethane in ether, obtained from *p*-toluenesulfonylmethylnitrosamide (2.14 g, 10 mmol).[72] Ether was evaporated, and two major products were separated by preparative GC.[73] The yields of methyl 1-(difluoromethyl)cyclobutane-1,3-dicarboxylate isomers were (cis) 80 mg (26%) and (trans) 15 mg (8%). Some **3** was recovered (30 mg, 7%). The structure of the cis isomer was determined by X-ray diffraction analysis on a crystal of the diacid,[15] obtained from **11** by hydrolysis with NaOH in aqueous methanol and further acidification with aqueous HCl.

Cis Isomer: ^{1}H NMR δ 6.12 (t, J = 56 Hz, 1H), 3.75 (s, 3H), 3.69 (s, 3H), 3.15 (p, J = 9 Hz, 1H), 2.73 (m, 2H), 2.57 (m, 2H); ^{19}F NMR δ −128.96 (d, J = 56 Hz); ^{13}C{^{1}H} NMR δ 27.43 (t, J = 4.4 Hz), 32.02 (s), 46.54 (t, J = 22.8 Hz), 52.04 (s), 52.75 (s), 115.94 (t, J = 234 Hz), 171.20 (t, J = 6.5 Hz), 174.41(s); EIMS *m*/*z* 223 (55) [M + 1]$^+$, 222 (21) M$^+$, 202 (9) [M − HF]$^+$, 191 (96), 170 (74), 163 (93), 143 (60), 131 (56), 115 (74), 105 (65), 85 (74), 77 (58), 59 (100), 55 (95), 51 (71); HRMS (calcd for $C_9H_{12}F_2O_4$ 222.0704) 222.0707.

Trans Isomer: ^{1}H NMR δ 6.02 (t, J = 56.4, 1H), 3.79 (s, 3H), 3.69 (s, 3H), 3.26 (p, J = 9Hz, 1H), 2.66 (m, 2H), 2.55 (m, 2H); ^{19}F NMR δ −128.23 (d, J = 56 Hz); ^{13}C{^{1}H} NMR δ 27.26 (t, J = 4.7 Hz), 31.92 (s), 46.92 (t, J = 26.3 Hz), 52.01 (s), 52.79 (s), 114.68 (t, J = 242.3 Hz), 171.99 (t, J = 5.1 Hz), 174.11(s); EIMS *m*/*z* 222 (2) M$^+$, 202 (1) [M − HF]$^+$, 191 (60), 170 (30), 162 (93), 143 (23), 131 (17), 115 (26), 111 (36), 105 (25), 85 (28), 71 (27), 59 (100), 55 (93), 51 (30); HRMS (calcd for $C_9H_{12}F_2O_4$ 222.0704) 222.0701.

Determination of pK_a Values of 4 and 24. Titrations were monitored by pH measurements with an Orion 81-72 Sure-Flow electrode and Orion 701A Ionalyzer. Aqueous solutions of **4** and of **24** (∼0.1 M; 20 mL) were titrated with an aqueous solution of NaOH (0.979 M). Readings of pH were recorded after addition of each ∼0.12 mL of NaOH solution. In one test experiment a basic solution after NaOH titration was titrated back with an aqueous solution of HCl (0.990 M). Nonlinear least-squares regression analysis of the volume of added NaOH solution and HCl solution as a function[74,75] of [H$^+$] yielded dissociation constants for the diacids. In all experiments the standard deviation of the fit $V = f([H^+])$[75] was below 5% of the mean value of V.

The conductance of aqueous solutions of **4** and of **24** and of their sodium salts (∼0.0001−0.1 M) was measured in a glass cell (cell constant ∼1) with platinum electrodes with a CV-50W voltammetric analyzer.[76] A potential step of 10 mV was applied to the cell with a solution, and the current was sampled at 54 and 72 μs after the step had been applied. The current decays exponentially, and the initial current was calculated by extrapolating to zero time. The measurement was performed 256 times for each solution, and the results were averaged.

Acknowledgment. The authors are grateful to Professors Petr Zuman (Clarkson University), Weston Borden (University

(69) An external capillary with a standard solution (10% of hexafluorobenzene in benzene-d_6, δ −163 ppm) was used to obtain lock and a reference signal in ^{19}F NMR measurements.

(70) EIMS for **8**: *m*/*z* 382 [M], 380 [M], 301 [M − Br], 255 [M − I], 253 [M − I], 174 [M − I − Br], 127 [I], 124, 93.

(71) When a large excess of SmI_2 is used, the intensity of the signal of **6** in ^{19}F NMR spectrum of the reaction mixture decreases, and a doublet (J = 1.6 Hz) δ −119.2 ppm appears in the spectrum. The mass spectrum of the new compound was assigned to **9**: *m*/*z* 302 [M], 175 [M − I], 155 [M − I − HF], 127 [I], 125, 113, 75.

(72) Furniss, B. S.; Hannaford, A. J.; Smith, P. W. G.; Tatchell, A. R. *Vogel's Textbook of Practical Organic Chemistry*, 5th ed.; Eds.; Longman: Essex, U.K., p 432.

(73) Column: 5% SE-52 on Chromosorb W, 21 feet long, 3/8 in. in diameter.

(74) (a) Reich, L. S.; Patel, S. H. *Am. Lab.* **1995**, *27*, 36. (b) Reich, L. S. *Am. Lab.* **1996**, *28*, 42.

(75) The equation used for nonlinear least-squares regression analysis for direct titration with aqueous NaOH was $V_b = \{V_aC_aK_1(2K_2 + [H^+])([H^+]^2 + K_1[H^+] + K_1K_2)^{-1} - V_a[H^+]\}(C_b + [H^+])^{-1}$, where V_b is the volume of added NaOH solution, V_a is the volume of the solution of the diacid before titration, C_a is the molar concentration of the diacid in solution before titration, C_b is the concentration of the NaOH solution, K_1 is the first dissociation constant, and K_2 is the second dissociation constant of the diacid. For the reverse titration with aqueous HCl the equation used was $V_t = \{V_aC_aK_1(2K_2 + [H^+])([H^+]^2 + K_1[H^+] + K_1K_2)^{-1} - V_b(C_b + [H^+]) - V_a[H^+]\}([H^+] - C_t)^{-1}$, where V_t is the volume of added HCl solution and C_t is the concentration of the HCl solution. In the derivation of the equations, terms containing the constant of dissociation of water were neglected since the diacids were strong.

(76) Bioanalytical Systems, Inc., 2701 Kent Ave., West Lafayette, IN 47906.

of Washington), and Tarek Sammakia (University of Colorado) for useful discussions. This research was supported by the National Science Foundation (Grants CHE-9318469, CHE-9412767, and CHE-9505926).

Supporting Information Available: Figure 4, details of the X-ray crystallographic analysis of **3** and **11**, views of the structure of the latter, spin-tickled ^{19}F NMR spectra of **2** and their interpretation, titration data for the diacids **4** and **24**, and optimized geometries for **13**, **14**, **21**, **23**, **25**, **27**, **28**, **29**, and some of the corresponding anions (62 pages). See any current masthead page for ordering and Internet access instructions.

JA9710518